Experimental and modeling studies of bicarbonate forming amines for CO_2 capture by NMR spectroscopy and VLE

Min Xiao[1,2], Ding Cui[2], Liangyu Zou[1], Qi Yang[2*], Hongxia Gao[1], Zhiwu Liang[1*]

[1]Joint International Center for CO_2 Capture and Storage (iCCS), Hunan Provincial Key Laboratory for Cost-effective Utilization of Fossil Fuel Aimed at Reducing CO_2 Emissions, College of Chemistry and Chemical Engineering, Hunan University, Changsha 410082, PR China

[2]CSIRO Manufacturing, Clayton, Victoria 3168, Australia

Corresponding author: Zwliang@hnu.edu.cn & Qi.yang@csiro.au

Abstract

Three tertiary diamines, *N*,*N*,*N*′,*N*′-tetramethyl-1,2-ethanediamine, *N*,*N*,*N*',*N*'-tetramethyl-1,3-propanediamine and *N*,*N*,*N*',*N*'-tetramethyl-1,4-butanediamine, were investigated for application in post-combustion CO_2 capture. The acid-base properties of the diamines were studied through measuring pH values of the acidified amine solutions to obtain reaction constants and corresponding enthalpies/entropies of the reactions. Competitive formation of monoprotonated and diprotonated diamines was observed. CO_2 absorption using these diamine solutions was carried out through a continuous flow method. NMR spectroscopy was used to detect speciation of the bulk solution. Then a general evaluation of the diamines was made in comparison with the monoamines in terms of equilibrium CO_2 solubility and p*Ka*. The results demonstrated the potential of the structurally modified diamines to be promising bicarbonate forming absorbents in CO_2 absorption. Finally, the equilibrium CO_2 solubility of aqueous *N*,*N*,*N*′,*N*′-tetramethyl-1,2-ethanediamine solution was measured at a wider range of temperatures, CO_2 partial pressures and initial amine concentrations to establish a thermodynamic model. The model provided reasonable prediction of equilibrium CO_2 solubility and species concentration profiles.

Key words: CO_2 capture; diamine; dissociation; equilibrium solubility; thermodynamic model.

1. Introduction

Increasing emissions of greenhouse gases, primarily CO_2 from human activities, is associated with global warming and climate change. Post-combustion carbon capture (PCC) is one of the most viable technologies to reduce CO_2 emissions until renewable energy is practical to replace fossil energy supplies[1, 2]. This technology has been studied for decades but obstacles still exist to restrict its commercialization. One of the key problems is the lack of appropriate absorbents to meet industrial requirements. Alkanolamine solvents are commonly used as the reactive absorbent in PCC for their high efficiency and good recyclability[3]. However, some problems such as a high energy penalty for regeneration and tendency for degradation are still unsolved. As a result, it is necessary to develop superior absorbents to substitute for the existingamine solvents.

Tertiary amine solutions are recognized as energy saving solvents in CO_2 capture. They promote the hydrolysis of CO_2 to form bicarbonate by a base-catalyzed mechanism instead of reacting with CO_2 directly[4], thus tertiary amine solutions have high CO_2 loading and can be easily regenerated. However, the hydrolysis of CO_2 is a much slower process compared with carbamate formation which only happens when primary or secondary amines are used.As such, activation is required to promote the CO_2absorption rate of tertiary amine solvents[5]. It is noticed that tertiary amines with different molecular structures can still vary significantly in their CO_2 capture performance[6], for example the CO_2 loading of diethylethanolamine is three times higher than that of triethanolamine[7], therefore, it is necessary to find more efficient

tertiary amines to improve the formulation of practical absorbents.

N,*N*,*N'*,*N'*-Tetramethylethylenediamine (TMEDA, C_2 backbone chain) provides a basic structural module to study diamines containing two tertiary amino groups to absorb CO_2. The goal is to improve the performance of amines by adding an additional amino group[8, 9]. This modification enables amine molecules to exhibit higher molecular efficiency with more active groups for CO_2 absorption. Since TMEDA only has tertiary amino group, it shows low energy penalty which is a typical advantage of tertiary amine. Our previous work suggested that the presence of hydroxyl group reduced both the CO_2 loading and the reaction rate of tertiary amines[10]. As TMEDA lacks a hydroxyl group, the diamine is expected to show better performance than the commonly studied alkanol tertiary amines such as triethanolamine (TEA) and *N*-methyldiethanolamine (MDEA). On the other hand, the absence of a hydroxyl group in an amine molecule may lead to poor water solubility which causes a lower amine concentration that is unfavorable in industrial applications due to lower energy efficiency. For TMEDA, the reduced water solubility due to the lack of hydroxyl group in comparison with MEA can be partially compensated by the additional amino group. The investigation of TMEDA as a preliminary example of amines with multiple tertiary amino groups shows a new direction to screen for superior tertiary amines. In order to demonstrate the potential of the tertiary diamines in CO_2 capture, the study of two TMEDA analogues, *N*,*N*,*N*',*N*'-tetramethyl-1,3-propanediamine (TMPDA, C_3 backbone carbon) and *N*,*N*,*N*',*N*'-tetramethyl-1,4-butanediamine (TMBDA, C_4 backbone carbon), are also

presented. These amines can be used as bicarbonate forming solvents to mix with other suitable additives for CO_2 capture[11, 12].

Whether being used as sole absorbent or formulated with activators in CO_2 absorption, tertiary amines only participate in protonation reactions. The performance of tertiary amines mainly depends on their acid-base properties. The pKa value of tertiary amine is more than a thermodynamic parameter as it also provides information about the kinetics of its protonation[13]. In the present case, the dissociation constants of the diamines TMEDA, TMPDA and TMBDA were obtained by measuring the pH of protonated amine solutions. Since the protonation and deprotonation of an amine are governed by temperature swing[14], the temperature dependence of the dissociation constant was investigated. Nuclear Magnetic Resonance (NMR) spectroscopy was used to measure the chemical shift variation of carbon peaks during the protonation process. Standard-state molar enthalpy (ΔH_m^0) and entropy (ΔS_m^0) of the protonation reaction were calculated via the van't Hoff equation, then the CO_2 absorption experiment was carried out using TMEDA, TMPDA and TMBDA solutions and speciation information on the bulk solutions was determined using NMR spectroscopy. The acid-base properties and equilibrium CO_2 solubility of those diamines were correlated to their molecular structure. The potential of using diamines as good absorbents in PCC was evaluated through comparison with monoamines. Finally, the solubility data of TMEDA solution was measured as a function of temperature, CO_2 partial pressure and initial amine concentration. Based on the vapor-liquid equilibrium (VLE) data, an activity coefficient model was applied

to the ternary TMEDA-H_2O-CO_2 system for thermodynamic analysis. The predictions on equilibrium CO_2 solubility and species concentration profiles were made for extended conditions.

2. Theory framework

2.1 Dissociation of protonated diamines

Since the reaction mechanism is quite similar for TMEDA, TMPDA and TMBDA, TMEDA is provided as an example here. The dissociation reaction of protonated TMEDA can be written as:

$$TMEDAH^+ \overset{K_1}{\leftrightarrow} TMEDA + H^+$$

$$TMEDAH_2^{2+} \overset{K_2}{\leftrightarrow} TMEDAH^+ + H^+$$

Two equations of equilibrium constant are generated from the dissociation reactions:

$$K_1 = \frac{[TMEDA][H^+]}{[TMEDAH^+]} \frac{\gamma_{TMEDA}\gamma_{H^+}}{\gamma_{TMEDAH^+}} \quad (1)$$

$$K_2 = \frac{[TMEDAH^+][H^+]}{[TMEDAH_2^{2+}]} \frac{\gamma_{TMEDAH^+}\gamma_{H^+}}{\gamma_{TMEDAH_2^{2+}}} \quad (2)$$

where $[i]$ and γ_i are the concentration and activity coefficient of species *i*, respectively; K_n is the equilibrium constant of reaction *n*. The equations are transformed to an expression of p*Ka* as:

$$pKa_1 = pH - \log\left(\frac{[TMEDA]}{[TMEDAH^+]}\right) - \log\left(\frac{\gamma_{TMEDA}}{\gamma_{TMEDAH^+}}\right) \quad (3)$$

$$pKa_2 = pH - \log\left(\frac{[TMEDAH^+]}{[TMEDAH_2^{2+}]}\right) - \log\left(\frac{\gamma_{TMEDAH^+}}{\gamma_{TMEDAH_2^{2+}}}\right) \quad (4)$$

The activity coefficient can be calculated from the Debye-Hückel equation:

$$\ln \gamma_i = - \frac{Az_i^2 I^{0.5}}{1+BI^{0.5}} (5)$$

where A is the Debye-Hückel constant as a function of temperature[15]; B can be given as an empirical value of 1.2 as suggested by Pitzer and Kim[16]; Z_i represents the charge on species i; I is ionic strength of the solution. Note that it is only valid for dilute solution to only consider the electrostatic force.

The ionic strength of solution I is written as:

$$I = \frac{1}{2}\sum[i]\,Z_i^2 \qquad (6)$$

The dissociation reaction of protonated TMEDA can be monitored via pH changes at different temperatures and the ratio of amine to protonated amine (or monoprotonated amine to diprotonated amine as shown in Equation 4).

2.2 Activity coefficient model for the TMEDA-CO_2-H_2O system

In the amine-CO_2-H_2O system, many other chemical reactions occur in the liquid phase besides amine protonation, such as hydrolysis of CO and bicarbonate dissociation. The system is much more complicated since various components are involved and mass transfer between the gas phase and the liquid phase is considerable. When CO_2 is absorbed intoTMEDA solution, there are three more reactions to be considered besides dissociation of protonated TMEDA:

$$CO_2 + H_2O \overset{K_3}{\leftrightarrow} HCO_3^- + H^+$$

$$H_2O \overset{K_4}{\leftrightarrow} H^+ + OH^-$$

$$HCO_3^- \overset{K_5}{\leftrightarrow} H^+ + CO_3^{2-}$$

These reactions give three equilibrium constants:

$$K_3 = \frac{[HCO_3^-][H^+]}{[CO_2]}\frac{\gamma_{HCO_3^-}\gamma_{H^+}}{\gamma_{CO_2}} \qquad (7)$$

$$K_4 = \frac{[H^+][OH^-]}{a_w}\gamma_{H^+}\gamma_{OH^-} \quad (8)$$

$$K_5 = \frac{[H^+][CO_3^{2-}]}{[HCO_3^-]}\frac{\gamma_{H^+}\gamma_{CO_3^{2-}}}{\gamma_{HCO_3^-}} \quad (9)$$

Since it is preferred to use high amine concentration to reduce energy, the short range van der Waals forces cannot be neglected. The activity coefficient is expressed using the extended Debye-Hückel equation:

$$\ln \gamma_i = -\frac{AZ_i^2\sqrt{I}}{1+B\sqrt{I}} + 2\sum \beta_{ij}[j] \quad (10)$$

where β_{ij} refers to the interaction parameter between species *i* and *j*. The expression is also valid for dissociation of protonated amine (Equations 1-2) at high concentration. The water activity, a_w, is set equal to the molar fraction.

The binary interaction parameter is regarded as a linear function of temperature:

$$\beta_{ij} = a_{ij} + b_{ij}T \quad (11)$$

where a_{ij} and b_{ij} areparameters to be estimated.

The two equations representing conservation of mass and the one denoting the charge balance can then be written as:

Mass balance of amine:

$$[TMEDA] + [TMEDAH^+] + [TMEDAH_2^{2+}] = [TMEDA]_t \quad (12)$$

Mass balance of carbon from CO_2:

$$[HCO_3^-] + [CO_2] + [CO_3^{2-}] = \alpha \times [TMEDA]_t \quad (13)$$

Charge balance:

$$[TMEDAH^+] + [H^+] + 2[TMEDAH_2^{2+}] = [HCO_3^-] + 2[CO_3^{2-}] + [OH^-] \quad (14)$$

where $[TMEDA]_t$ is the initial concentration of TMEDA and α represents equilibrium CO_2 solubility.

The concentration of CO_2 in the liquid phase is calculated from its partial pressure via Henry's law:

$$P_{CO_2} \times \emptyset_{CO_2} = He \times [CO_2] \times \gamma_{CO_2} \quad (15)$$

where P_{CO_2} is CO_2 partial pressure, $\emptyset_{CO_2}$ is the CO_2fugacity coefficient, He is Henry's law constant for CO_2.

3. Experimental section

3.1 Materials

CO_2 and N_2 were purchased from Changsha RIZHENG Gas Co., Ltd. TMEDA (99%, Acros Organics), TMPDA (99%, Acros Organics), TMBDA (97%, Merck) were used as purchased. TMEDA (99%, Aladdin Industrial Corporation) was used as received in the VLE experiments. The abbreviations and molecular structures of diamines used in this study are shown in Figure 1. Deionized water was used to dissolve the amines. Titration with standard sodium hydroxide was used to verify lab-prepared hydrochloric acid solution concentration (0.70 M). A thermostatic water-circulator (HX20, Shanghai Hannuo Instruments Co. Ltd), mass flow controller (D07, Beijing Sevenstar Electronics Co. Ltd.), pH meter (pH 110, OAKTON Instruments connected with InLab NMR pH electrode with accuracy of ± 0.01) and NMR spectrometer (Bruker Avance III 400MHz spectrometer) were used in experiments. An external reference capillary of 13% trioxane in D_2O was added to each NMR tube to assist the signal lock during acquisition and the calibration of the chemical shift (C: 93.52 ppm). The conditions for quantitative ^{13}C NMR analysis are the same as described in the work of Li *et al*[17]. The data processing was carried out

using Bruker TopSpin 3.5 software.

3.2 Methods

3.2.1 Determination of dissociation constant

Thirty samples were prepared by mixing different amounts of HCl into diamine solutions, similar to the work of Yu *et al*[18]. The concentration of diamine was fixed in each sample solution at 0.05 $mol \cdot L^{-1}$. The concentration of HCl was varied from 0 to 0.12 $mol \cdot L^{-1}$ to give a range of acid/diamine concentration ratios from 0 to 2.4 (since 2 HCl molecules are required per diamine molecule). The samples were maintained in a thermally controlled water bath for more than 10 minutes at the planned temperature (298, 303, 308, 318 and 333 K) before pH values were measured. NMR spectra were recorded at 298 K.

3.2.2 CO_2 absorption

The CO_2 absorption was carried out in a continuous flow reactor. A mixture of CO_2 and $N_2$was controlled using mass flow controllers to adjust the CO_2 partial pressure to 15 kPa. The overall flow rate of the mixed gas was 50 $mL \cdot min^{-1}$. After being saturated with water, the simulated flue gas was bubbled through 15 mL of 2.0 $mol \cdot L^{-1}$ diamine solutions in the reactor. The temperature of the system was maintained at 313 K using a temperature-controlled water bath and the solution stirred at 900 rpm with a magnetic stirring bar. Samples were taken from the bulk solution at specific times for quantitative ^{13}C NMR analysis. The CO_2 absorption experiment was carried out for

five hours. The diagram of the continuous flow reactor is shown in Figure 2.

3.2.3 Measurement of VLE data

The equilibrium CO_2 solubility of TMEDA, TMPDA and TMBDA solutions were measured under the same conditions as in the CO_2absorption experiment described above (CO_2 15kPa, 298K) with prolonged absorption time of 24 hours. The equilibrium CO_2 solubility measurement of TMEDA was extended to a wider range of CO_2 partial pressures (15, 30, 60 and 101 kPa), absorbing temperatures (293, 313 and 333 K) and initial amine concentrations (1.0, 3.0 and 5.0 $mol \cdot L^{-1}$). Samples were taken under each set of conditions to measure CO_2 solubility using Chittick apparatus until the system reached equilibrium and no CO_2 solubility change was observed. A detailed description of the Chittick apparatus and analysis process can be found in our previous work[10].

4. Results and discussion

4.1 Dissociation constant of protonated diamines

Since the two amino groups in the studied diamines are identical, the protonation reaction of these diaminesonly generates two forms of protonated molecules, monoprotonated and diprotonated. During the acidification of the diamine solutions, two equivalence points at HCl/amineconcentration ratio of 1.0 and 2.0 are expected. The titration curve of TMEDA in Figure 3 shows two rapid decreases of pH at these ratios, corresponding to monoprotonation and diprotonation at these points

respectively. As only a C2 carbon chain lies between the two active nitrogen atoms of TMEDA, the electrostatic repulsion effect of monoprotonated TMEDA will significantly reduce the activity of the second nitrogen atom[19]. This is the why two distinct equivalence points are observed. On the other hand, the titration curves of TMPDA and TMBDA only show one significant pH value decrease around the HCl/amineconcentration ratio of 2.0. These observations are correlated to the increased backbone carbon chain length from C_2 to C_3 and C_4, leading to the reduced influence of the electrostatic repulsion effect. The second protonation, therefore, may happen before the completion of the first one, and only one equivalence point is observed.

The correlation of electrostatic repulsion effect with the change of the backbone chain lengths is further supported by NMR analysis. A series of ^{13}CNMR spectra of TMEDA solution are stacked in S-Figure 1 in the supplementary material showing how the chemical shift changes with the HCl/amine concentration ratio. The signals with chemical shifts around 44.1 ppm and 55.4 ppm are due to the carbon-1' and the carbon-1 of TMEDA respectively. Since there exists fast proton exchange among amine species $Amine/AmineH^+/AmineH_2^{2+}$, the signals of the free amine are not distinguishable from those of its protonated forms. For the convenience of result analysis, the changes in ^{13}C NMR chemical shifts of the measured samples of TMEDA, TMPDA and TMBDA are displayed in Figure 4 and the vertical lines are provided to guide the eye. For TMEDA, the change in chemical shift of carbon-1 is linear when plotted against the HCl/amine ratio in the range from 0 to 2.0, when all

nitrogen atoms are protonated and there is no further response to the change of acid/baseratio. The chemical shift of carbon-1'showsa different responseto the protonation reaction:the trend is a linear up to an HCl/amine ratio of 1.0, however the curve slope changes after this point. The changes of curve slope are also observed for TMPDA and TMBDA but less distinct due to the stronger second protonation.

The calculation of pKa_1 and pKa_2 values for the diamines can be divided into two separate parts according to acid/base ratio, one is from zero to 1.0 and the other from 1.0 to 2.0. The calculations of p$Ka_1$and pKa_2 of TMEDA at 298 K are displayed in Table 1 and Table 2 respectively as examples. The calculated values (9.28 of pKa_1 and5.89 ofpKa_2) agree well with literature values of 9.281 and 6.130[20]. The pKa_1 and pKa_2 of TMEDA, TMPDA and TMBDA was further studied as a function of temperature from 298 to 333 K as shown in Figure 5 (values are provided in the supplementary material, S-Table 1). To quantify the standard-state molar enthalpies (ΔH_m^0) and entropies (ΔS_m^0) of the reaction, the pKa linked to the dissociation constant is then correlated with temperature using the van't Hoff equation (16):

$$\ln K = -\ln 10^{pKa} = -\frac{\Delta H^0}{RT} + \frac{\Delta S^0}{R} \qquad (16)$$

The molar standard-state free energy ΔG_m^0 can be calculated as:

$$\Delta G^0 = \Delta H^0 - T\Delta S^0 \qquad (17)$$

The thermodynamic properties of TMEDA, TMPDA and TMBDA are given in Table 3 together with that of MDEA, TEA and TREA (triethylamine) obtained from the literature[21].The positive enthalpies ΔH_m^0 of dissociation of monoprotonated and diprotonated diamines prove that the reactions are endothermic. The relatively small

entropies ΔS_m^0 indicate that the reactions are mainly determined by enthalpy, therefore heat is required to deprotonate the ammonium ions when the solution is loaded with CO_2. It is found that the dissociation enthalpies of monoprotonated diamine increase with the backbone chain length as 33.79, 39.91 and 40.69 $kJ \cdot mol^{-1}$for TMEDA, TMPDA and TMBDA respectively. All of these values are higher than the dissociation enthalpy of TEA (22.72 $kJ \cdot mol^{-1}$) and MDEA (34.92 $kJ \cdot mol^{-1}$) but lower than that of TREA (45.6 $kJ \cdot mol^{-1}$). The higher enthalpies indicates that the dissociation reaction is more sensitive to the temperature change. The enthalpies of diprotonated diamine dissociation are lower than that of monoprotonated diamine dissociation but show similar trend as: TMEDA (30.73 $kJ \cdot mol^{-1}$) < TMPDA (37.11 $kJ \cdot mol^{-1}$) < TMBDA (40.17 $kJ \cdot mol^{-1}$). It is pointed out that the deviation between enthalpies of dissociation of monoprotoanted and diprotonated diamines reduces with the increase of chain length.

4.2 Species profiles of protonation

The protonation process of diamine solutions was simulated based on the above theory framework to give concentration profiles over a range of HCl/amine ratios from 0.0 to 2.0. The chemical model incorporates Equations 1, 2, 5, 6, 8, amine balance Equation 12, and charge balance Equation 14 where the concentration of bicarbonate and carbonate was eliminated in this calculation. Initially the pH values were predicted and compared to the measured pH titrations to demonstrate the robustness of the method. Good agreement was observed between the measured and

predicted pH values with average deviation of 1.2%. Calculated species concentration profiles are shown in Figure 6.

The Figure 6(a) shows the predicted concentration profiles of the free, monoprotonated and diprotonated diamines versus HCl/amine ratio. A negative correlation of free diamine and a positive correlation of diprotonated diamine were observed with increasing HCl/amine ratio. The concentrations of monoprotonated diamine increase to a maximum value at acid/base ratio of 1.0 and then decrease with the increase of acid/base ratio. The simulated data supports with the observations from NMR spectra. In addition, the concentrations of the diprotonated species $TMBDAH_2^{2+}$, $TMPDAH_2^{2+}$ and $TMEDAH_2^{2+}$ start to increase around HCl/amine ratios of 0.5, 0.75 and 1.0, respectively. The overlap of free and diprotonated amine curves in this region leads to an obvious reduction of the peak concentration of monoprotonated diamine products in the order: $TMBDAH^+ < TMPDAH^+ < TMEDAH^+$. This is consistent with the previous assumption that the smaller deviation between dissociation constants of monoprotonated and diprotonated diamines, as a consequence of the longer backbone chain length, will promote the competitiveness of diprotonation and bring forward the formation of diprotonated amine.

The concentration profiles of proton and hydroxide during protonation are displayed Figure 6(b). Higher hydroxide concentration is related to higher pKa. The proton concentration in TMEDA solution starts to increase much more rapidly than that in TMPDA and TMBDA solution at acid/base concentration ratio of 1.0,

indicating a significant decrease of pH. The proton concentration curves of TMPDA and TMBDA follow the same pattern as that of TMEDA solution but it cannot be well displayed in the figure due to a much lower concentration range.

4.3 CO_2 absorption

The CO_2 absorption of TMEDA, TMPDA and TMBDA was studied using NMR spectroscopy. We have only presented the detailed NMR results for TMEDA here as they are representative of all three diamines, which have a similar absorption mechanism. In the stacked ^{13}C NMR spectra of CO_2 loaded TMEDA solutions (S-Figure 2), a new signal appears around 162.1 – 160.4 ppm as the CO_2 loading increases. This peak is due to the formation of HCO_3^-/CO_3^{2-}. With increasing CO_2 loading, the chemical shifts of the TMEDA carbons swing towards the higher magnetic field due to the protonation reaction. This chemical shift swing and the absence of a carbamate signal confirms that TMEDA only participates in protonation reactions. The chemical shift is plotted in Figure 7 against CO_2 loading. No obvious inflection point occurs in the curves before the equilibrium state. This provides evidence that the monoprotonation reaction dominates the whole CO_2 absorption process whereas the diprotonation reaction of $TMEDAH^+$contributes little in CO_2 absorption. The concentration of major species in CO_2 loaded TMEDAsolution can be calculated using the information from the NMR spectra. The respective concentrations of HCO_3^- and CO_3^{2-} can be calculated using the following equations[9]:

$$[HCO_3^-] = \frac{168.03 - \delta}{168.03 - 160.3} \times \alpha \times [TMEDA]_t \qquad (18)$$

$$[CO_3^{2-}] = \frac{\delta - 160.3}{168.03 - 160.3} \times \alpha \times [TMEDA]_t \qquad (19)$$

Meanwhile, an approximate charge balance equation is:

$$[TMEDAH^+] = [HCO_3^-] + 2[CO_3^{2-}] \qquad (20)$$

where some components such as H^+, OH^- and $TMEDAH_2^{2+}$ are ignored due to their much lower concentration. The results calculated from the experimental data are plotted as points in Figure 8. They show that the concentration of TMEDA decreases and that of HCO_3^- and $TMEDAH^+$ increase with increasing CO_2 loading. Meanwhile, CO_3^{2-} is always presents as a minor species in the dynamic conversion of carbonate/bicarbonate. Its concentration steadily increases until the CO_2 loading reaches 0.331 mol CO_2·mol amine^{-1}. At high CO_2 loading range, the concentration of CO_3^{2-} is found to decrease.

4.4 Equilibrium CO_2 solubility

Equilibrium CO_2 solubility is an essential criterion for the evaluation of amine performance for PCC. The equilibrium CO_2 solubility and p*Ka* of TMEDA, TMPDA and TMBDA are compared with monoamines to demonstrate the potential of using diamine with dual tertiary amino groups in CO_2 capture. The chemical structures of the other amines are shown in the supplementary material, S-Figure 3. In Figure 9, a linear trend between p*Ka* and equilibrium CO_2 solubility is observed for amines containing one tertiary amino group, which correlates stronger bases to higher equilibrium CO_2 solubility[10, 21-27]. The point representing the first protonation of

TMEDA lies near the linear trend line of the monoamines as little contribution is made from the second tertiary amino group in the molecule. It is found that both the pKa_1 value and equilibrium CO_2 solubility of TMEDA are higher than those of triethanolamine (TEA), methyldiethanolamine (MDEA) and dimethylethanolamine (DMEA). The molecular structure is mainly responsible for the variation as multiple hydroxyl groups reduce the pKa and equilibrium CO_2 solubility of both TEA and MDEA. The comparison of TMEDA and DMEA further demonstrates that the replacement of the hydroxyl group with a tertiary amino groupimproves those properties. Other factors, besides the number of hydroxyl groups, will also affect the basicity of the amine, such as the position of the hydroxyl group and the presence of a strong electron donating group. Some tertiary amines, e.g. 4-diethylamino-2-butanol (DEAB) containing one hydroxyl group spaced by a C3 chain from amino group, and triethylamine (TREA) which has no hydroxyl groups, show better performance than TMEDA. It is noted that the poor water solubility and low boiling point of TREA restricts its application in CO_2 capture. It is used in this study for comparison of the influence of amine structures only, as it has ahigh pKa value resulting from three electron-donating ethyl groups.

The analogues of TMEDA with a longer backbone chain length, TMPDA and TMBDA, show a much higher pKa due to the reduction of electrostatic repulsion effect[28]. It is also noted that the increment of pKa_2 is larger than pKa_1. The increased activities of the second tertiary amino group of TMPDA and TMBDA leads to a significant increase of equilibrium CO_2 solubility to give an order of TMEDA

(0.754 mol CO_2·mol amine^{-1}) < TMPDA (1.171 mol CO_2·mol amine^{-1}) < TMBDA (1.448 mol CO_2·mol amine^{-1}). In addition, the water solubility of diamines is promising on account of the two amino groups. The low boiling point of TMEDA (121℃) can be overcome by increasing the chain length (145℃ of TMPDA and 166℃ of TMBDA). Lower regeneration energy cost is expected since CO_2 only exists as carbonate and bicarbonate in the CO_2-loadedsolution. This demonstrates the potential of di-tertiary amines to have high molecular efficiency through an appropriate modification as the amines with multiple proton acceptors can be good bicarbonate forming promoters in CO_2 capture. However, the chemical stability of those di-tertiary amines under practical conditions needs to be further investigated. The amine degradation behaviour may result in solvent loss, by-products accumulation, foaming, corrosion which have significant influence to CO_2 capture performance.

4.5 Thermodynamic model of ternaryamine-H_2O-CO_2 system

Thermodynamic modeling provides a comprehensive analysis of the equilibrium amine-CO_2-H_2O system as a function of component composition and temperature[29]. The correlation and prediction capability of the thermodynamic model is of interest for process design and simulation. Herein, a thermodynamic model is established using the C2 backbone chain diamine, TMEDA.

4.5.1 Equilibrium CO_2 solubility data of TMEDA solution

The equilibrium CO_2 solubility of TMEDA was measured at wider conditions to

investigate the influence of experimental conditions (the data aresummarized in supplementary material, S-Tables 2-4). Increase of CO_2 partial pressure leads to higher equilibrium CO_2 solubility. Based on Henry's law, higher CO_2 partial pressure creates stronger driving force for the reactions in solution, thus resulting in more dissolved CO_2. A negative correlation between the equilibrium CO_2 solubility and temperature was observed due to the exothermic behavior of CO_2 absorption. The equilibrium CO_2 solubility also shows a negative correlation to amine concentration. Although more CO_2in total can be absorbed in an amine solution of a higher concentration, the equilibrium CO_2 solubility (measured as mol CO_2:mol diamine) decreased for amine solutions with higher concentration.

4.5.2 Model development

An activity coefficient model, namely Deshmukh-Mather model, is used to simulate the equilibrium TMEDA-CO_2-H_2O system[30].The constants applied in the model are summarized in Table 4, in which dissociation constants K_1 and K_2 are obtained in this work and the other constants such as reaction constants (K_3, K_4 and K_5),Henry's law constant (*He*),and the Debye-Hückel constant (*A*) are extracted from literature[31, 32]. CO_2 fugacity can be calculated using the Peng-Robinson equation of state[33]. The computation is briefly described below: VLE data were input to calculate all required constants and fugacity. Initial values for the concentration of eight unknown species in the liquid phase were obtained by solving Equations 1, 2 and 6-15 simultaneously, where the activity coefficients were calculated without the

second term, then interaction parameters were generalized from the optimization of all equations. Although there were many possible interaction parameters in the liquid phase, only the most important interactionsbetween high concentration species ($TMEDA - HCO_3^-$, $TMEDAH^+ - HCO_3^-$ and $TMEDA - TMEDAH^+$) were considered[30]. The interactions of species such as $TMEDAH_2^{2+}$, CO_2, CO_3^{2-}, H^+ and OH^- were neglected due to their exceedingly low concentrations and insignificant contribution to the second term of Equation 10. The prediction of equilibrium CO_2 solubility was made by inputting some necessary parameters (temperatures, CO_2 partial pressures, initial amine concentrations and interaction parameters) while equilibrium solubility α was to be solved. A calculated value of α was obtained from optimization of Equations 1, 2 and 6-15, then iteration was applied to optimize the concentration of eight species and three pairs of interaction parameters (β_{ij}) until the objective function (OF) was minimized to an acceptable value. The objective function is expressed as:

$$\mathrm{OF} = \sum \left| \frac{\alpha_{exp} - \alpha_{cal}}{\alpha_{exp}} \right| \qquad (18)$$

where α_{exp} is the experimental equilibrium CO_2 solubility and α_{cal} represents the calculated equilibrium CO_2solubility. The final results of optimized interaction parameters are tabulated in Table 5.

4.5.3 Model predictions

The predicted equilibrium CO_2 solubility of TMEDA solutions are compared with experimental data to give a reasonable prediction with an average deviation of 8.4%.

The speciation of CO_2 absorption using TMEDA solution is also predicted based on the thermodynamic model. The computation is similar to the prediction of equilibrium CO_2 solubility, except CO_2 partial pressure is set as the unknown parameter. For the convenience of comparison to the experimental data, the prediction is provided under the amine concentration of 2.0 mol·L^{-1} and temperature of 313 K. The prediction results are integrated in Figure 8 to show that the calculated concentrations of all components in TMEDA solution fit well with the data obtained from the NMR analysis. In Figure 8, the concentration of $TMEDAH_2^{2+}$ is low before CO_2 loading of 0.754 mol CO_2·mol $amine^{-1}$ which supports the previous conclusion that protonation of the second amino group makes little contribution in CO_2 absorption. When it approaches the saturation point in solution most TMEDA has been monoprotonated, then the second protonation reaction starts and the concentration of $TMEDAH_2^{2+}$ increases, however 0.754 mol CO_2·mol $amine^{-1}$ is the maximum experimental CO_2 loading value obtained under the given experimental conditions. Increasing CO_2 partial pressure is required to obtain higher CO_2 loading, therefore the curve of $[CO_2]$ (proportional to CO_2 partial pressure according to Henry's law) begins to be visible at high CO_2 loading as shown in Figure 8. It is noted that the CO_2 partial pressure increases dramatically at this region, implying the dominant driving force changes from chemical absorption to physical absorption.

5. Conclusions

Investigation of the dissociation reaction of protonated diamines TMEDA, TMPDA

and TMBDA revealed the competition between monoprotonation and diprotonation of the diamines. The equilibrium CO_2 solubility, determined by NMR, and p*Ka* of TMEDA, TMPDA and TMBDA were evaluated in comparison with monoamines to expose the correlation of structure features such as functional group, backbone chain length and hydroxyl group to the amine activities in CO_2 absorption. This comparison highlighted the potential of diamines with multiple proton acceptors as alternative absorbents to promote bicarbonate formation. The equilibrium CO_2 solubility of TMEDA solution were measured under a wide range of temperatures, CO_2 partial pressures and amine concentrations, and a thermodynamic model was developed which gave good predictions on equilibrium CO_2 solubility and species concentration profiles.

Acknowledgment:

Financial support from the National Natural Science Foundation of China (NSFC-Nos. 21536003, 21706057, 21776065, 21606078, 21476064 and 51521006), the National Key Technology R&D Program (MOST-No. 2014BAC18B04), the China Outstanding Engineer Training Plan for Students of Chemical Engineering & Technology in Hunan University (MOE-No.2011-40), the Opening Project of Guangxi Colleges and Universities Key Laboratory of Beibu Gulf Oil and Natural Gas Resource Effective Utilization (2016KLOG17, 2016KLOG13, 2016KLOG11 and 2016KLOG05), Hunan Provincial Innovation Foundation for Postgraduate (CX2017B135) and the China Scholarship Council (201706130044) are gratefully

acknowledged. The authors are also very grateful for the CISRO PhD student scholarship to support this research. Dr. R. Mulder and Dr J. Cosgriff are gratefully acknowledged for their assistance with NMR experiments.

Literature cited

[1] G.T. Rochelle, Amine Scrubbing for CO_2 Capture, Science, 325 (2009) 1652-1654.
[2] A.V. Rayer, K.Z. Sumon, T. Sema, A. Henni, R.O. Idem, P. Tontiwachwuthikul, Part 5c: Solvent chemistry: solubility of CO_2 in reactive solvents for post-combustion CO_2, Carbon Manage., 3 (2012) 467-484.
[3] N.E. Hadri, D.V. Quang, E.L.V. Goetheer, M.R.M.A. Zahra, Aqueous amine solution characterization for post-combustion CO_2 capture process, Applied Energy, 185 (2017) 1433-1449.
[4] T.L. Donaldson, Y.N. Nguyen, Carbon Dioxide Reaction Kinetics and Transport in Aqueous Amine Membranes, Ind. Eng. Chem. Fundam., 19 (1980) 260-266.
[5] R. Zhang, X. Zhang, Q. Yang, H. Yu, Z. Liang, X. Luo, Analysis of the reduction of energy cost by using MEA-MDEA-PZ solvent for post-combustion carbon dioxide capture (PCC), Applied Energy, 205 (2017) 1002-1011.
[6] G. Puxty, R. Rowland, A. Allport, Q. Yang, M. Bown, R. Burns, M. Maeder, M. Attalla, Carbon Dioxide Postcombustion Capture: A Novel Screening Study of the Carbon Dioxide Absorption Performance of 76 Amines, Environ. Sci. Technol., 43 (2009) 6427-6433.
[7] M. Xiao, H. Liu, H. Gao, Z. Liang, CO_2 absorption with aqueous tertiary amine solutions: Equilibrium solubility and thermodynamic modeling, J. Chem. Thermodynamics, 122 (2018) 170-182.
[8] B. Yu, H. Yu, K. Li, Q. Yang, R. Zhang, L. Li, Z. Liang, Characterisation and kinetic study of carbon dioxide absorption by an aqueous diamine solution, Applied Energy, 208 (2017) 1308-1317.
[9] R. Zhang, Q. Yang, B. Yu, H. Yu, Z. Liang, Toward to efficient CO_2 capture solvent design by analyzing the effect of substituent type connected to *N*-atom, Energy, 144 (2018) 1064-1072.
[10] M. Xiao, H. Liu, R. Idem, P. Tontiwachwuthikul, Z. Liang, A study of structure-activity relationships of commercial tertiary amines for post-combustion CO_2 capture, Applied Energy, 184 (2016) 219-229.
[11] A. Hartono, R. Rennemo, M. Awais, S.J. Vevelstad, O.G. Brakstad, I. Kim, H.K. Knuutila, Characterization of 2-piperidineethanol and 1-(2-hydroxyethyl)pyrrolidine as strong bicarbonate forming solvents for CO_2 capture, Int. J. Greenh. Gas Control, 63 (2017) 260-271.

[12] A. Hartono, S.J. Vevelstad, A. Ciftja, H.K. Knuutila, Screening of strong bicarbonate forming solvents for CO_2 capture, Int. J. Greenh. Gas Control, 58 (2017) 201-211.
[13] H. Liu, Z. Liang, T. Sema, W. Rongwong, C. Li, Y. Na, R. Idem, P. Tontiwachwuthikul, Kinetics of CO_2 Absorption into a Novel 1-Diethylamino-2-propanol Solvent Using Stopped-Flow Technique, AIChE J., 60 (2014) 3502-3510.
[14] D. Fernandes, W. Conway, X. Wang, R. Burns, G. Lawrance, M. Maeder, G. Puxty, Protonation constants and thermodynamic properties of amines for post combustion capture of CO_2, J. Chem. Thermodynamics, 51 (2012) 97-102.
[15] A. Benamor, M.K. Aroua, Modeling of CO_2 solubility and carbamte concentration in DEA, MDEA and their mixtures using the Deshmukh-Mather model, Fluid Phase Equilibria, 231 (2005) 150-162.
[16] K.S. Pitzer, J.J. Kim, Thermodynamics of Electrolytes. IV. Activity and Osmotic Coefficients for Mixed Electrolytes, J. Am. Chem. Soc., 96 (1959) 5701-5707.
[17] X. Li, Q. Yang, P. Pearson, B. Yu, G. Puxty, D. Xiao, The application of trans-1,4-diaminocyclohexane as a bicarbonate formation rate promoter in CO_2 capture, Fuel, 226 (2018) 479-489.
[18] B. Yu, L. Li, H. Yu, M. Maeder, G. Puxty, Q. Yang, P. Feron, W. Conway, Z. Chen, Insights into the Chemical Mechanism for CO_2(aq) and H^+ in Aqueous Diamine Solutions - An Experimental Stopped-Flow Kinetic and $^1H/^{13}C$ NMR Study of Aqueous Solutions of N,N-Dimethylehtylenediamine for Postcombustion CO_2 Capture, Environ. Sci. Technol., 52 (2018) 916-926.
[19] A. Bencini, A. Bianchi, E. Garcia-Espana, M. Micheloni, J.A. Ramirez, Proton coordination by polyamine compounds in aqueous solution, Coord. Chem. Rev., 188 (1999) 97-156.
[20] P. Paoletti, R. Barbucci, A. Vacca, A. Dei, Thermodynamics of protonation of amines. Values of log *K*, *ΔH*, and *ΔS* for the Protonation of *NN*'- and *NN*-Dimethylethylenediamine and *NNN'N'*-Tetramethylethylenediamine, J. Chem. Soc. (A). 0 (1971) 310-313.
[21] A.V. Rayer, K.Z. Sumon, L. Jaffari, A. Henni, Dissociation Constants (p*Ka*) of Tertiary and Cyclic Amines: Structural and Temperature Dependences, J. Chem. Eng. Data, 59 (2014) 3805-3813.
[22] R.J. Littel, M. Bos, G.J. Knoop, Dissociation Constants of Some Alkanolamines at 293, 303, 318 and 333 K, J. Chem. Eng. Data, 35 (1990) 276-277.
[23] K. Maneeintr, R.O. Idem, P. Tontiwachwuthikul, A.G.H. Wee, Synthesis, Solubilities, and Cyclic Capacities of Amino Alcohols for CO_2 Capture from Flue Gas Streams, Energ Procedia, 1 (2009) 1327-1334.
[24] H. Liu, M. Li, R. Idem, P. Tontiwachwuthikul, Z. Liang, Analysis of solubility, absorption heat and kinetics of CO_2 absorption into 1-(2-hydroxyethyl)pyrrolidine solvent, Chem. Eng. Sci., 162 (2017) 120-130.
[25] H. Liu, T. Sema, Z. Liang, K. Fu, R. Idem, Y. Na, P. Tontiwachwuthikul, CO_2 absorption kinetics of 4-diethylamine-2-butanol solvent using stopped-flow technique, Sep. Sci. Technol., 136 (2014) 81-87.

[26] H. Liu, M. Xiao, Z. Liang, W. Rongwong, J. Li, P. Tontiwachwuthikul, Analysis of Reaction Kinetics of CO_2 Absorption into a Novel 1-(2-Hydroxyethyl)-piperidine Solvent Using Stopped-Flow Technique, Ind. Eng. Chem. Res., 54 (2015) 12525-12533.
[27] S. Kadiwala, A.V. Rayer, A. Henni, Kinetics of carbon dioxide (CO_2) with ethylenediamine, 3-amino-1-propanol in methanol and ethanol, and with 1-dimethylamino-2-propanol and 3-dimethylamino-1-propaonl in water using stopped-flow technique, Chem. Eng. J., 179 (2012) 262-271.
[28] R. Zhang, Q. Yang, Z. Liang, G. Puxty, R.J. Mulder, J.E. Cosgriff, H. Yu, X. Yang, Y. Xue, Toward Efficient CO_2 Capture Solvent Design by Analyzing the Effect of Chain Lengths and Amino Types to the Absorption Capacity, Bicarbonate/Carbamate, and Cyclic Capacity, Energy & Fuels, 31 (2017) 11099-11108.
[29] G. Puxty, M. Maeder, A simple chemical model to represent CO_2-amine-H_2O vapour-liquid-equilibria, Int. J. Greenh. Gas Control, 17 (2013) 215-224.
[30] R.D. Deshmukh, A.E. Mather, A mathematical model for equilibrium solubility of hydrogen sulfide and carbon dioxide in aqueous alkanolamine solutions, Chem. Eng. Sci., 36 (1981) 355-362.
[31] T.J. Edwards, G. Maurer, J. Newman, J.M. Prausnitz, Vapor-Liquid Equilibria in Multicomponent Aqueous Solutions of Volatile Weak Electrolytes, AIChE J., 24 (1978) 966-976.
[32] C.-C. Chen, H.I. Britt, J.F. Boston, L.B. Evans, Extension and Application of the Pitzer Equation for Vapor-Liquid Equilibrium of Aqueous Electroyte Systems with Molecular Solutes, AIChE J., 25 (1979) 820-831.
[33] D.-Y. Peng, D.B. Robinson, A New Two-Constant Equation of State, Ind. Eng. Chem. Fundam., 15 (1976) 59-64.

Figure captions

Figure 1. Abbreviations and molecular structures of amines investigated

Figure 2. Diagram of the continuous flow reactor

Figure 3. pH *vs* HCl/amine concentration ratio at 298 K

Figure 4. Changes of ^{13}C NMR chemical shift of protonated TMEDA, TMPDA and TMBDA

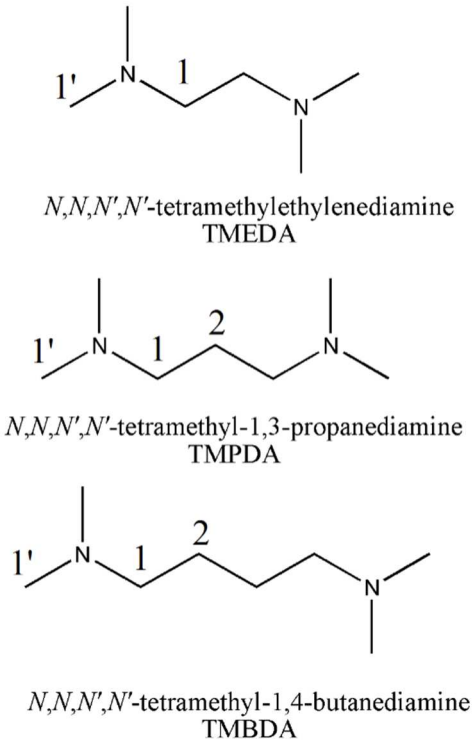

Figure 1. Abbreviations and molecular structures of amines investigated

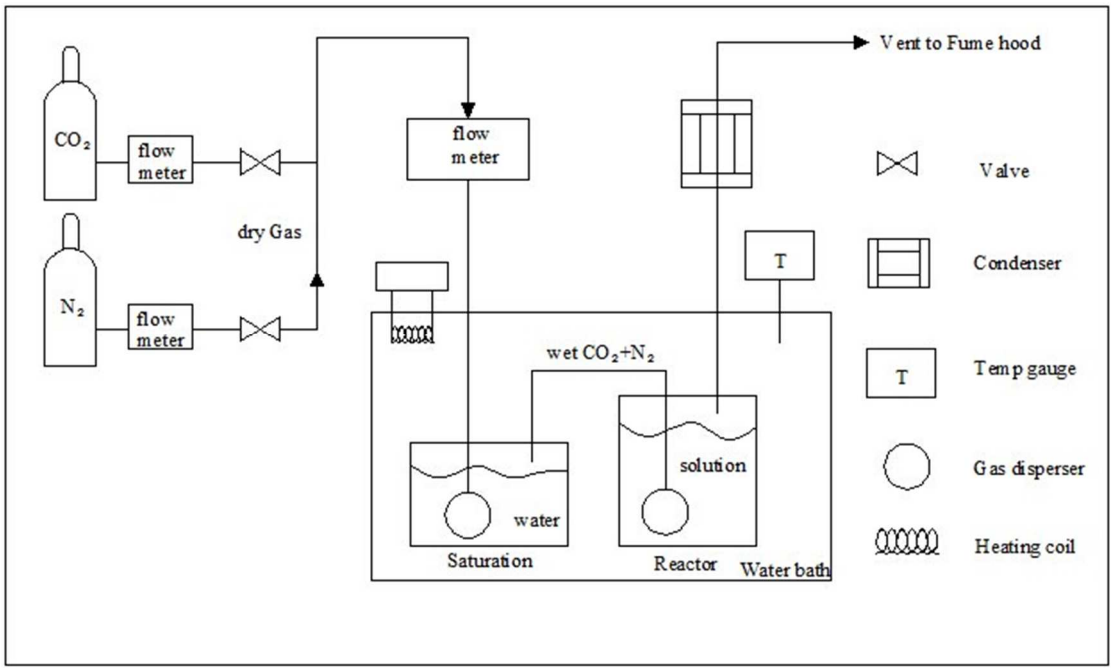

Figure 2. Diagram of the continuous flow reactor

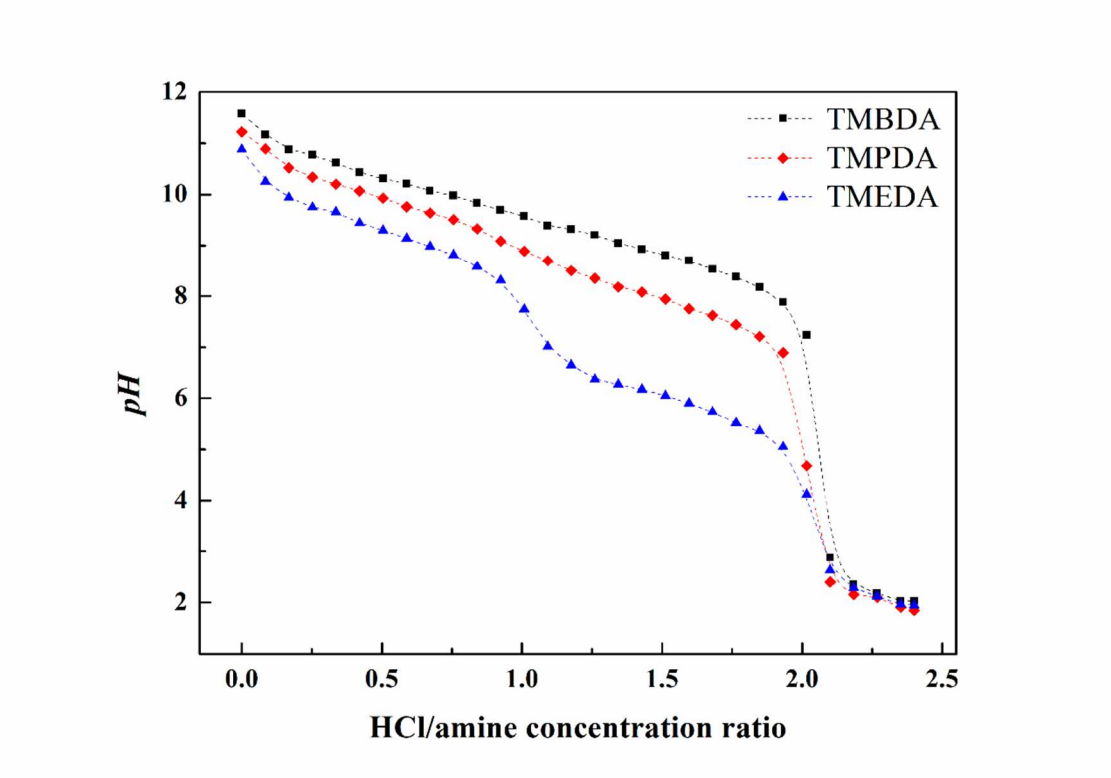

Figure 3. pH *vs* HCl/amine concentration ratio at 298 K

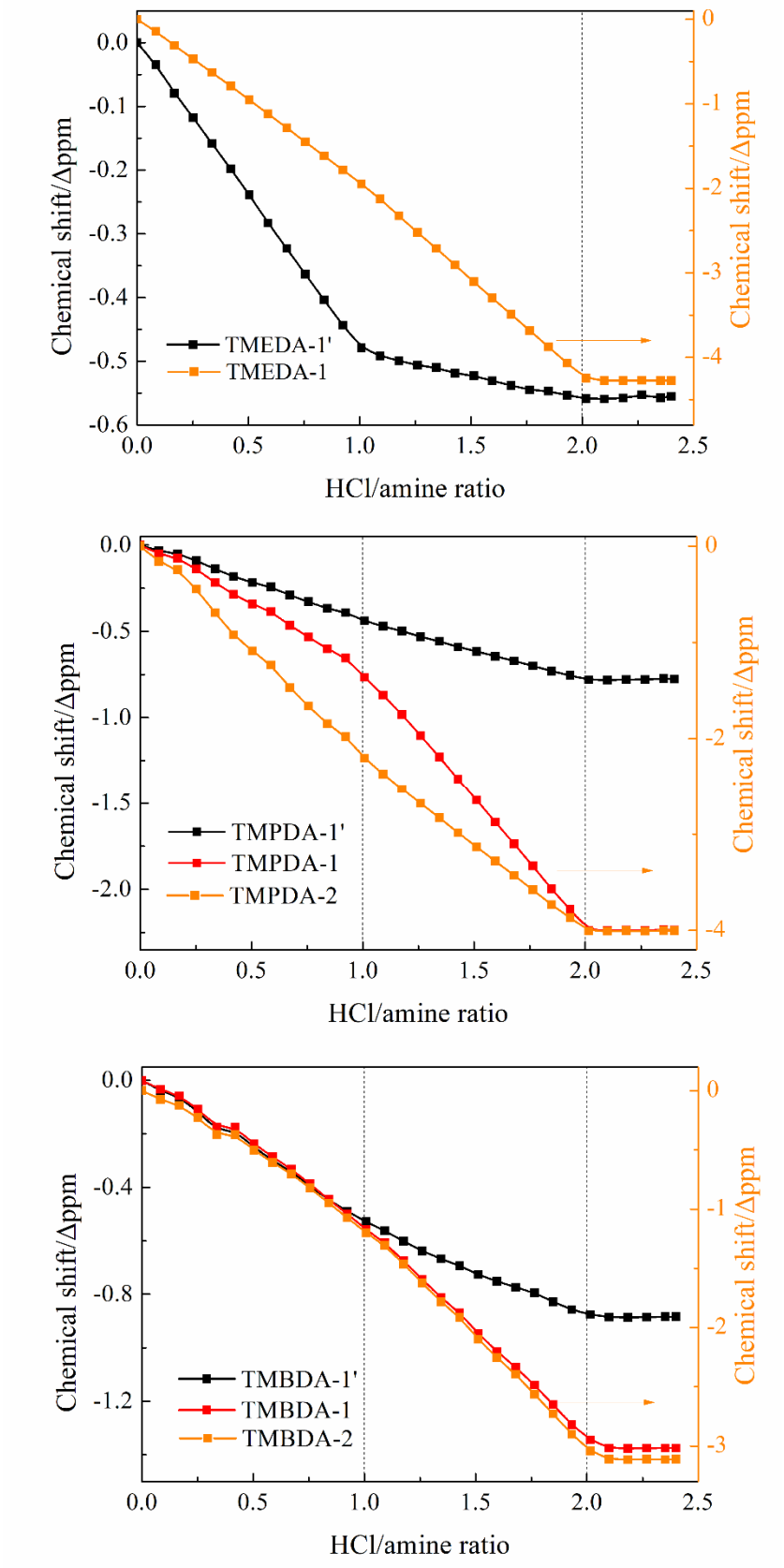

Figure 4. Changes of ^{13}C NMR chemical shift of protonated TMEDA, TMPDA and TMBDA

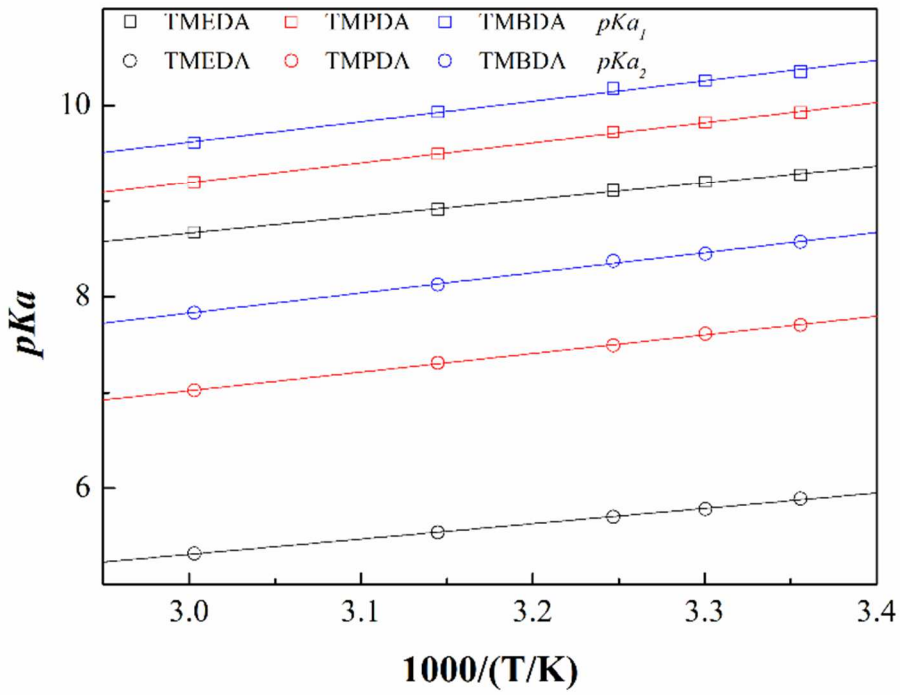

Figure 5. pK_a of TMEDA, TMPDA and TMBDA as a function of temperatures

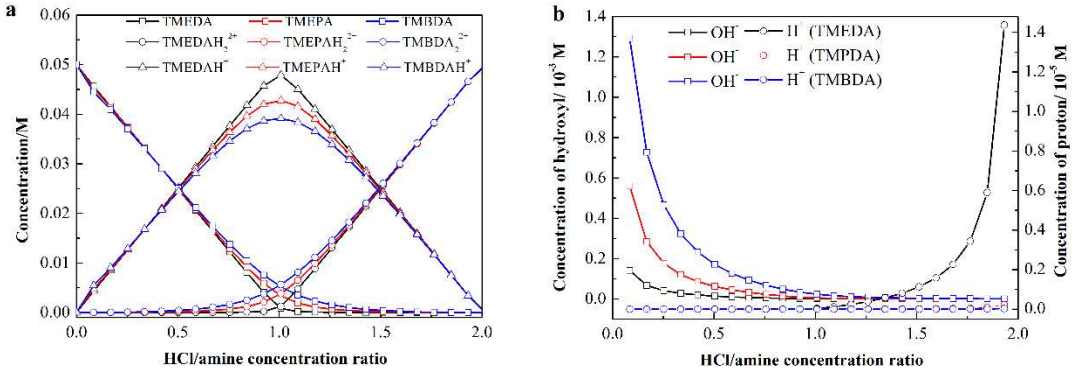

Figure 6. Concentration profiles of diamine solutions at HCl/amine concentration ratio from zero to 2.0

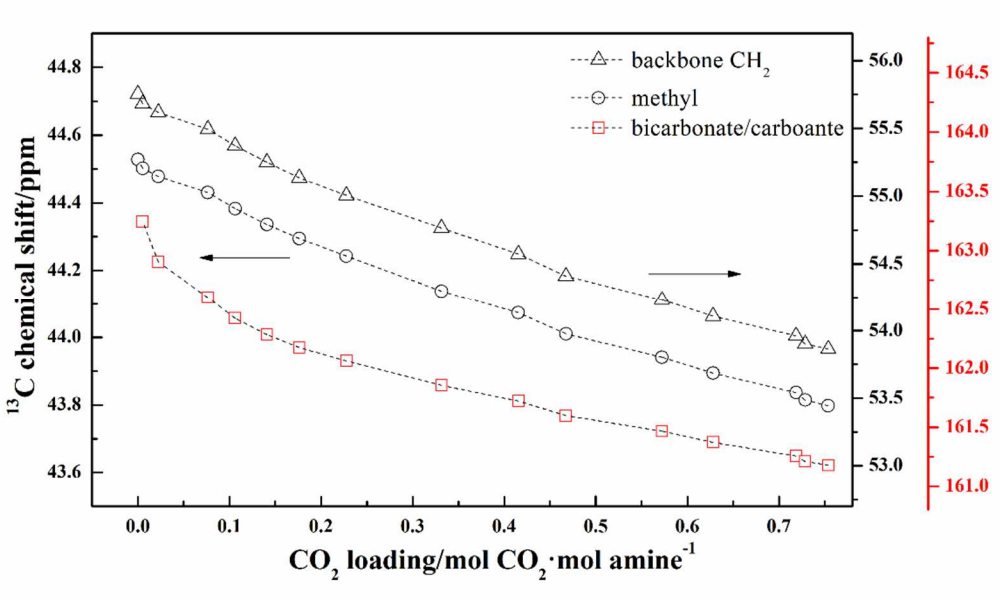

Figure 7. ^{13}C Chemical shift of TMEDA solution for CO_2 absorption

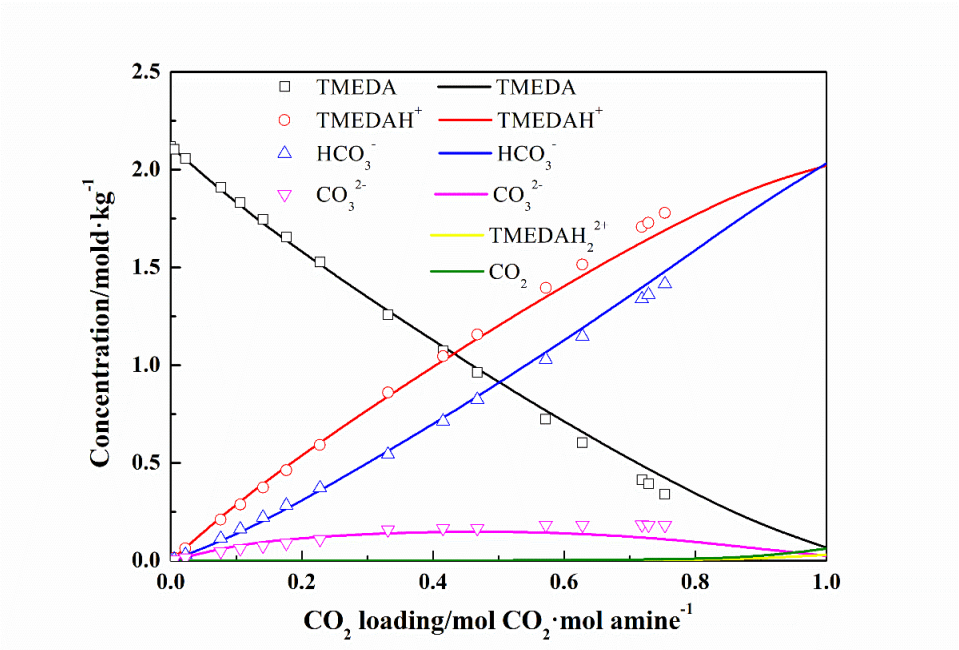

Figure 8. Speciation plot of CO_2 absorption using 2.0 mol·L^{-1} (2.119 mol·kg^{-1}) TMEDA solution, where points are experimental data and curves are predicted from the model

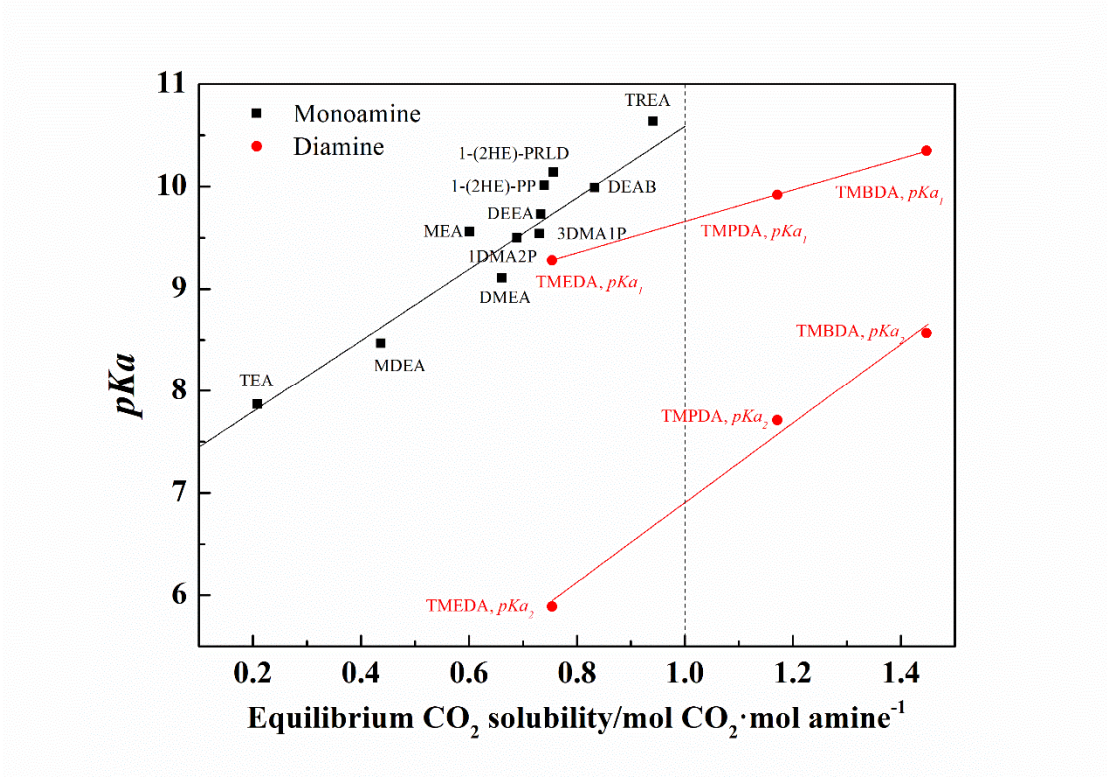

Figure 9. Comparison of amines in terms of p*Ka* (at 298 K) and equilibrium CO_2 solubility (at 313 K, 2.0 mol·L^{-1} and 15 kPa, except TREA)

Table Captions

Table 1. Calculation of pKa_1 for TMEDA

Table 2. Calculation of pKa_2 for TMEDA

Table 3. Thermodynamic properties for the amine dissociation reaction

Table 4. Constant expressions of K_n, He and A(in mol·kg^{-1} basis)

Table 5. Binary interaction parameters β_{ij} for the TMEDA-H_2O-CO_2 system

Table 1. Calculation of pKa_1 for TMEDA

Ratio of [HCl] to [amine]	pH	$\log\left(\frac{[TMEDA]}{[TMEDAH^+]}\right)$	$\log\left(\frac{\gamma_{TMEDA}}{\gamma_{TMEDAH^+}}\right)$	pKa_1
0.00	10.88	N/A	N/A	N/A
0.08	10.25	1.04	0.01	9.20
0.17	9.94	0.69	0.01	9.23
0.25	9.75	0.47	0.02	9.27
0.34	9.66	0.30	0.02	9.35
0.42	9.44	0.14	0.02	9.28
0.50	9.30	-0.01	0.02	9.29
0.59	9.14	-0.15	0.02	9.28
0.67	8.98	-0.31	0.03	9.27
0.76	8.82	-0.49	0.03	9.29
0.84	8.58	-0.72	0.03	9.28
0.92	8.31	-1.08	0.03	9.37
Average value in this work				9.28
Literature value [20]				9.281

Table 2. Calculation of pKa_2 for TMEDA

Ratio of [HCl] to [amine]	pH	$\log\left(\frac{[TMEDAH^+]}{[TMEDAH_2^{2+}]}\right)$	$\log\left(\frac{\gamma_{TMEDAH^+}}{\gamma_{TMEDAH_2^{2+}}}\right)$	pKa_2
1.01	7.74	2.09	0.09	5.56
1.09	7.01	0.99	0.10	5.92
1.18	6.65	0.67	0.10	5.88
1.26	6.37	0.45	0.11	5.81
1.34	6.27	0.28	0.11	5.88
1.43	6.17	0.13	0.11	5.93
1.51	6.05	-0.02	0.12	5.95
1.60	5.90	-0.17	0.12	5.95
1.68	5.73	-0.33	0.12	5.93
1.76	5.52	-0.51	0.13	5.90
1.85	5.36	-0.75	0.13	5.98
1.93	5.05	-1.14	0.13	6.05
Average value in this work				5.89
Literature value [20]				6.130

Table 3. Thermodynamic properties for the amine dissociation reaction

Amine	ΔG_m^0/kJ·mol^{-1}	ΔH_m^0/kJ·mol^{-1}	ΔS_m^0/kJ·mol^{-1}·K^{-1}	Source
TMEDA, Equation 1	53.00	33.79	-0.06	this work
TMEDA, Equation 2	33.56	30.73	-0.01	this work
TMPDA, Equation 1	56.69	39.91	-0.06	this work
TMPDA, Equation 2	43.99	37.11	-0.02	this work
TMBDA, Equation 1	59.19	40.69	-0.06	this work
TMBDA, Equation 2	48.93	40.17	-0.03	this work
MDEA	49.88	34.92	-0.05	[21]
TEA	45.17	22.72	-0.07	[21]
TREA	61.75	45.6	-0.05	[21]

Table 4. Constant expressions of K_n, He and A(in mol·kg^{-1} basis)

Constant expressions	Source
$K_1 = \exp(-\frac{4064.3}{T} - 7.752)$	this work
$K_2 = \exp(-\frac{3696.6}{T} - 1.1398)$	this work
$K_3 = \exp(235.482 - \frac{12092.1}{T} - 36.7816 \ln T)$	[31]
$K_4 = \exp(140.932 - \frac{13445.9}{T} - 22.4773 \ln T)$	[31]
$K_5 = \exp(220.067 - \frac{12431.7}{T} - 35.4819 \ln T)$	[31]
$He = \exp\left(94.4914 - \frac{6789.04}{T} - 11.4519 \ln T - 0.010454T\right) \times 101.32$	[31]
$A = -1.306568 + 0.01328238T - (0.3550803\mathrm{E}-4)T^2 + (0.3381968\mathrm{E}-7)T^3$	[32]

Table 5. Binary interaction parameters β_{ij} for the TMEDA-H_2O-CO_2 system

Species interaction	a_{ij}(kg·mol^{-1})	b_{ij}(kg K·mol^{-1})
TMEDA - $TMEDAH^+$	-1.576	5.628E-03
TMEDA - HCO_3^-	-0.170	4.775E-04
$TMEDAH^+$ - HCO_3^-	0.393	-1.008E-03